N72-28684

NASA TECHNICAL MEMORANDUM

NASA TM X-68097

NASA TM X-68097

CASE FILE COPY

A SHIELDING APPLICATION OF PERTURBATION THEORY TO DETERMINE CHANGES IN NEUTRON AND GAMMA DOSES DUE TO CHANGES IN SHIELD LAYERS

by Daniel Fieno
Lewis Research Center
Cleveland, Ohio

TECHNICAL PAPER proposed for presentation at
National Topical Meeting on New Development in Reactor
Physics and Shielding sponsored by the
American Nuclear Society
Kiamesha Lake, New York, September 12-15, 1972

E-7070

A SHIELDING APPLICATION OF PERTURBATION THEORY TO DETERMINE CHANGES IN NEUTRON AND GAMMA DOSES DUE TO CHANGES IN SHIELD LAYERS

by Daniel Fieno

Lewis Research Center
National Aeronautics and Space Administration
Cleveland, Ohio

ABSTRACT

Perturbation theory for fixed sources was applied to radiation shielding problems to determine changes in neutron and gamma ray doses due to changes in various shield layers. For a given source and detector position the perturbation method enables dose derivatives due to all layer changes to be determined from one forward and one inhomogeneous adjoint calculation. The direct approach requires two forward calculations for the derivative due to a single layer change. Hence, the perturbation method for obtaining dose derivatives permits an appreciable savings in computation for a multilayered shield. For an illustrative problem, a comparison was made of the fractional change in the dose per unit change in the thickness of each shield layer as calculated by perturbation theory and by successive direct calculations; excellent agreement was obtained between the two methods.

INTRODUCTION

Reactors for space propulsion systems or auxiliary power systems require shielding to protect personnel, system components, or payload from neutrons and gamma radiation. These shields are usually composed of alternate layers of heavy metal and hydrogeneous material. The shielding problem for these systems is to determine the number, arrangement, and thicknesses of these shield layers that will result in minimum weight shields while maintaining the radiation field at various positions around the system within prescribed limits.

One-dimensional shield weight optimization procedures have been evolved for the design of layered configurations (refs. 1, 2, 3) and these have been extended to constraints in several directions around two-dimensional configurations (refs. 3, 4, 5). All of these require the determination of the change in dose at a detector due to a change in thickness of each layer of a given shield configuration. These are generally obtained with S_N transport calculations requiring at least as many separate calculations as there are shield layers. As the optimization proceeds and the configuration changes, this procedure has to be repeated until the configuration converges to an optimum one. The optimization procedure beoomes time consuming and particularly for the two-dimensional case

would require excessive amounts of computer time.

The present work applies perturbation theory for systems with fixed sources to this shielding problem. The perturbation method utilizes only one forward and one inhomogeneous adjoint solution for an initially selected layered shield configuration to determine all necessary dose derivatives at a detector for a given neutron or gamma ray source component. The method appreciably reduces the amount of calculation required for multilayered shields. In addition, perturbation theory yields a considerable amount of information concerning the effect of various physical processes (elastic scatter, inelastic scatter, etc.) on the dose rate.

The perturbation method in this work is applied to a simple spherical system to determine the dose derivatives of the various layers. This illustrative problem also serves to demonstrate the ability of the perturbation method to extract additional informative data concerning interaction processes of the various shield materials.

ANALYSIS

The theory underlying the application of perturbation methods to non-reactivity problems appears mainly in the Russion nuclear energy literature (refs. 6 and 7). Lewins reviews in reference 8 developments in perturbation theory. This section presents the equations used in the perturbation analysis for systems with fixed sources. The theory will be outlined for a fixed source neutron system since the results for fixed source gamma ray system are similar in form.

Consider the time-independent multigroup form of the inhomogeneous neutron transport equation. This equation is given by

$$\vec{\Omega}\cdot\vec{\nabla}\phi_g(\vec{r},\vec{\Omega}) + \sigma_g(\vec{r})\phi_g(\vec{r},\vec{\Omega}) = Q_g(\vec{r},\vec{\Omega}) + \sum_{\ell=0}^{\infty}\frac{2\ell+1}{4\pi}\sum_{g'}\sigma_\ell(\vec{r},g'\to g)\sum_{m=-\ell}^{\ell}\phi_{\ell,m}^{g'}(\vec{r})\,P_{\ell,m}(\vec{\Omega})\,;$$
$$g = 1, 2, \ldots\ldots G. \tag{1}$$

The notation used for equation (1) is conventional: $\phi_g(\vec{r},\vec{\Omega})$ is the angular flux for group g, σ_g is the macroscopic total cross section for group g, $Q_g(\vec{r},\vec{\Omega})$ is the angular fixed source distribution for group g, $\sigma_\ell\,(g'\to g)$ is the ℓ-th order expansion coefficient of the scattering from group g' to group g, $\phi^g_{\ell,m}(\vec{r})$ is the ℓ,m-th expansion coefficient of the angular flux in a spherical harmonics series, and $P_{\ell,m}(\vec{\Omega})$ is the ℓ,m-th spherical harmonic as a function of the unit vector $\vec{\Omega}$. The boundary condition for the angular flux

at the convex boundary of the system is taken as

$$\phi_g(\vec{r}_s, \vec{\Omega}^-) = 0 \;;\quad g = 1, 2, \ldots G \tag{2}$$

This boundary condition is the usual condition implying that no neutrons enter the system from the vacuum. Here $\vec{r}_s$ indicates the outer boundary of the system and $\vec{\Omega}^-$ designates an inwardly directed direction $\vec{\Omega}$.

Once the solution to equation (1) has been obtained, then a physical process which depends linearly on the angular flux may be written as a functional F. The multigroup form of F is given by

$$F = \sum_g \iint \phi_g(\vec{r},\vec{\Omega})\, P_g(\vec{r},\vec{\Omega})\, d\vec{r}\, d\Omega \tag{3}$$

The functional F gives contributions caused by the interaction process for the neutrons in the system. The quantity $P_g(\vec{r},\vec{\Omega})$ has the role of an interaction cross section for group g at position $\vec{r}$ for neutrons moving in the direction $\vec{\Omega}$.

Following Usachev (ref. 6) an equation can be derived for the importance of neutrons for the physical process described by the functional F. This equation for the importance $\psi_g(\vec{r},\vec{\Omega})$ which is equal to the effect F at some detector position or region due to a unit source of neutrons placed in group g at $(\vec{r},\vec{\Omega})$, is given in multigroup form by

$$\begin{aligned} -\vec{\Omega}\cdot\vec{\nabla}\psi_g(\vec{r},\vec{\Omega}) &+ \sigma_g(\vec{r})\psi_g(\vec{r},\vec{\Omega}) = P_g(\vec{r},\vec{\Omega}) \\ &+ \sum_{\ell=0}^{\infty} \frac{2\ell+1}{4\pi} \sum_{g'} \sigma_\ell(\vec{r}, g\to g') \sum_{m=-\ell}^{\ell} \psi_{\ell,m}^{g'}(\vec{r})\, P_{\ell,m}(\vec{\Omega}) \;; \\ & g = 1, 2, \ldots G, \end{aligned} \tag{4}$$

The boundary condition for the importance $\psi_g(\vec{r},\vec{\Omega})$ follows from the fact that, if a neutron escapes from a system, it cannot contribute to the physical process of interest. Therefore its importance must be zero and the boundary condition becomes

$$\psi_g(\vec{r}_s, \vec{\Omega}^+) = 0 \;,\quad g = 1, 2, \ldots G \tag{5}$$

where $\vec{\Omega}^+$ designates an outwardly directed direction $\vec{\Omega}$.

The next step in the analysis is to derive a perturbation equation in terms of a perturbation in the density of the material constituents of the system. The perturbation in the density of a material, which can be related to a perturbation in the thickness of a given shielding layer, is introduced in the equations through the macroscopic cross sections and appears as a perturbation in the cross sections of the system. The solution of equation (1) with the perturbed cross sections yields a perturbed value for the angular flux $\mathcal{F}(\vec{r},\vec{\Omega})$. The equation for the perturbed system is

$$\vec{\Omega}\cdot\vec{\nabla}\mathcal{F}_g(\vec{r},\vec{\Omega}) + [\sigma_g(\vec{r})+\delta\sigma_g(\vec{r})]\,\mathcal{F}_g(\vec{r},\vec{\Omega}) = Q_g(\vec{r},\vec{\Omega}) + \delta Q_g(\vec{r},\vec{\Omega})$$

$$+ \sum_{\ell=0}^{\infty}\frac{2\ell+1}{4\pi}\sum_{g'}\left[\sigma_\ell(\vec{r},g'\to g)+\delta\sigma_\ell(\vec{r},g'\to g)\right]\sum_{m=-\ell}^{\ell}\mathcal{F}^{g'}_{\ell,m}(\vec{r})\,P_{\ell,m}(\vec{\Omega});$$

$$g = 1, 2, \ldots G \tag{1a}$$

along with the boundary condition

$$\mathcal{F}_g(\vec{r}_s,\vec{\Omega}^-) = 0\ ; \quad g = 1, 2, \ldots G \tag{2a}$$

In the above equation $\mathcal{F}(\vec{r},\vec{\Omega})$ represents the perturbed value of the angular flux for group g. Perturbations in the cross sections are indicated by $\delta\sigma$. Also the source term $Qg(\vec{r},\vec{\Omega})$ is assumed to undergo a perturbation in the amount of $\delta\,Qg(\vec{r},\vec{\Omega})$.

The neutron transport equation for the perturbed system, equation (1a), along with the equation for the importance can be manipulated to give the following result:

$$\sum_g\int_{\vec{\Omega}} d\Omega\int d\vec{r}\;\delta\sigma_g(\vec{r})\,\psi_g(\vec{r},\vec{\Omega})\,\mathcal{F}_g(\vec{r},\vec{\Omega})$$

$$-\sum_{\ell=0}^{\infty}\frac{2\ell+1}{4\pi}\sum_{m=-\ell}^{\ell}\int d\vec{r}\,\sum_{g'}\mathcal{F}^{g'}_{\ell,m}(\vec{r})\sum_{g}\delta\sigma_\ell(\vec{r},g'\to g)\,\psi^{g}_{\ell,m}(\vec{r})$$

$$-\sum_g\int_{\vec{\Omega}} d\Omega\int d\vec{r}\;\psi_g(\vec{r},\vec{\Omega})\left[Q_g(\vec{r},\vec{\Omega})+\delta Q_g(\vec{r},\vec{\Omega})\right]$$

$$+\sum_g\int_{\vec{\Omega}} d\Omega\int d\vec{r}\;\mathcal{F}_g(\vec{r},\vec{\Omega})\,P_g(\vec{r},\vec{\Omega}) = 0 \tag{6}$$

Equation (6) is an exact relationship and represents a condition which the perturbed angular flux and importance must satisfy. If all of the perturbations in equation (6) are zero, then the equation reduces to

$$F = \sum_g \int_{\vec{\Omega}} d\Omega \int d\vec{r}\, \phi_g(\vec{r},\vec{\Omega})\, P_g(\vec{r},\vec{\Omega})$$

$$= \sum_g \int_{\vec{\Omega}} d\Omega \int d\vec{r}\, \psi_g(\vec{r},\vec{\Omega})\, Q_g(\vec{r},\vec{\Omega}) \qquad (3a)$$

Where $\mathfrak{F}_g(\vec{r},\vec{\Omega})$ has been replaced by its unperturbed value $\phi_g(\vec{r},\vec{\Omega})$. The result expressed by equations (3 & 3a) is well known.

In the perturbed systems the functional F^P giving the contributions for the physical process of interest is equal to

$$F^P = \sum_g \iint \mathfrak{F}_g(\vec{r},\vec{\Omega})\, P_g^P(\vec{r},\vec{\Omega})\, d\vec{r}\, d\Omega \qquad (7)$$

Here the general case of a perturbed system is considered for which $P_g^P(\vec{r},\vec{\Omega})$ is the perturbed value of the quantity $P_g(\vec{r},\vec{\Omega})$. The quantity $P_g^P(\vec{r},\vec{\Omega})$ is taken to be

$$P_g^P(\vec{r},\vec{\Omega}) = P_g(\vec{r},\vec{\Omega}) + \delta P_g(\vec{r},\vec{\Omega}) \qquad (8)$$

Next consider the difference δF of the functionals F^P and F. Using equations (3a), (7) and (8) in equation (6) results in

$$\begin{aligned}
\delta F = &- \sum_g \int_{\vec{\Omega}} d\Omega \int d\vec{r}\, \delta\sigma_g(\vec{r})\, \psi_g(\vec{r},\vec{\Omega})\, \mathfrak{F}_g(\vec{r},\vec{\Omega}) \\
&+ \sum_{\ell=0}^{\infty} \left(\frac{2\ell+1}{4\pi}\right) \sum_{m=-\ell}^{\ell} \int d\vec{r} \sum_{g'} \mathfrak{F}_{\ell,m}^{g'}(\vec{r}) \sum_g \delta\sigma_\ell(\vec{r}, g'\to g)\, \psi_{\ell,m}^{g}(\vec{r}) \\
&+ \sum_g \int_{\vec{\Omega}} d\Omega \int d\vec{r}\, \psi_g(\vec{r},\vec{\Omega})\, \delta Q_g(\vec{r},\vec{\Omega}) \\
&+ \sum_g \int_{\vec{\Omega}} d\Omega \int d\vec{r}\, \mathfrak{F}_g(\vec{r},\vec{\Omega})\, \delta P_g(\vec{r},\vec{\Omega})
\end{aligned} \qquad (9)$$

Equation (9) is the desired perturbation expression for a system with fixed sources. This equation gives the change in the functional F for a given physical

process due to changes in various neutron cross sections, changes in the fixed source, and changes in the physical process itself. Equation (9) is an exact relationship since no approximations are inherent in its derivation. However, since only first order perturbation theory is being considered, the perturbed flux $\mathfrak{F}_g(\vec{r},\vec{\Omega})$ may be replaced by its unperturbed value $\phi_g(\vec{r},\vec{\Omega})$.

In shielding analysis, generally the biological dose rate at a detector position $\vec{r}_d$ is the functional of greatest interest. The interaction cross sections $P_g(\vec{r},\vec{\Omega})$ are the flux to dose conversion factors which are independent of $\vec{\Omega}$. Thus, we can express $P_g(\vec{r},\vec{\Omega})$ as

$$P_g(\vec{r},\vec{\Omega}) = \frac{d_g}{4\pi}\,\delta(\vec{r}-\vec{r}_d) \qquad \ldots(10)$$

where dg is the flux to dose conversion factor for group g and $\delta(\vec{r}-\vec{r}_d)$ is the Dirac delta function. Insertion of equation (10) into equation (3) gives

$$F = \frac{1}{4\pi}\sum_g d_g\,\Phi_g(\vec{r}_d) \qquad \ldots(11)$$

Thus the functional F is $(1/4\pi)$ times the dose rate at position $\vec{r}_d$.

ILLUSTRATIVE PROBLEM

The spherical system chosen for this study shown in figure 1 has a central cavity or void region with a radius of 30 centimeters. This void region is followed by a 15 centimeter thick layer of natural tungsten and a 60 centimeter thick layer of lithium hydride. The dimensions and composition of this system are listed in Table I.

The neutron dose was calculated using 26 energy groups at a detector located 0.25 centimeters from the outer boundary of the system. This group structure is shown in Table II. The fixed neutron source of 1.7×10^{17} neutron/sec was uniformly distributed in the central void region. The neutron fluxes and importances were determined using the S_n method with elastic scattering treated through the P_3 order and using an S_{16} Gauss-Legendre angular quadrature. The effect on the neutron dose as measured at the detector position was then determined for tungsten and lithium hydride for all the important neutron reactions by using the perturbation formula given by equation (9). The results obtained with the perturbation formula are for a nominal perturbation in the density of each layer.

The total effect of the tungsten or lithium hydride layer can be expressed as the fractional change in the neutron dose functional per unit change in layer thickness. These quantities are compared with similar results obtained from

successive direct flux calculations in which a nominal change in the density (or equivalently thickness) of a layer is made.

Neutron interactions with tungsten nuclei generate a secondary source of gamma rays throughout the tungsten layer. The secondary gamma ray sources are due to the W(n,γ) and W(n, n'γ) reactions. Results for these two secondary gamma ray sources will be presented separately. The analysis and results obtained for these secondary gamma ray sources follows that presented for the fixed source neutron problem; however, perturbations in the secondary source due to perturbations in the W(n,γ) and W(n,n'γ) reactions caused by perturbations in the W density must also be included. All of the gamma ray calculation were obtained using the group structure given in Table III and for an S_{16} Gauss-Legendre angular quadrature with scattering treated through the P_3 order.

RESULTS

Effect of the Tungsten and Lithium Hydride Layers on the Neutron Dose

The neutron dose rate was calculated from equation (3) to be 2.90 x 10^2 rem/hr for the source of 1.7 x 10^{17} neutrons/sec. The neutron dose calculated using equation (3a) was computed to be 3.11 x 10^2 rem/hr. The ratio of the dose calculated from equations (3a) and (3) was equal to 1.07. This ratio should be unity and departure from unity is a measure of the approximations inherent in the S_n method for a given spatial mesh and angular quadrature. Thus, if the values of the dose functional differ by a large enough amount to preclude obtaining the accuracy desired, then S_n calculated angular fluxes and importance must be recalculated with a finer spatial mesh and angular quadrature. For the illustrative problem being considered, the error in the perturbation results is approximately half the percent difference in the values of the two dose functionals.

Table IV presents the effect on the neutron dose functional, $4\pi\delta F$, of the tungsten layer. The data in Table IV gives the effect on $4\pi\delta F$ of each reaction which a neutron can undergo with nuclei of tungsten. Inelastic neutron scattering accounts for 60.9 percent of the contribution to the total $4\pi\delta F$; elastic neutron scattering contributes 19.6 percent; (n,2n) reactions contribute 18.8 percent; and neutron absorptions contributes 0.7 percent. The data in Table IV indicates, as an example, that a 1 percent increase in the density of the tungsten layer would decrease the dose of 2.90 x 10^2 rem/hr at the detector position by 10.3 rem/hr. Also given in Table IV is the change in the neutron dose functional per gram of material. A value of -2.00 x 10^{-4} rem/hr/gm was obtained for W. Table IV also gives the change in the neutron dose functional per centimeter. For natural tungsten this coefficient is -68.9 rem/hr/cm.

Table V gives a comparison of the fractional change in the neutron dose functional per unit change in the W layer thickness, $\delta F/F\delta t$ between the perturbation theory result and the result calculated by successive direct transport calculations. The perturbation theory result is -.238 cm^{-1} while the result from direct

flux calculations is -.234 cm^{-1}. The two results are in excellent agreement with each other.

Table VI presents the effect on the neutron dose functional, $4\pi\delta F$, of the lithium-hydride layer. In addition, partial effects due to constituents H and Li are also presented. Table VI indicates the dominant role of elastic neutron scattering for low mass number elements on the dose functional. The data in Table VI shows that a 1 percent increase in the lithium-hydride density would decrease the dose of 2.90 x 10^2 rem/hr at the detector position by 24.0 rem/hr; hydrogen and lithium contribute 12.2 and 11.8 rem/hr, respectively, of the 24.0 rem/hr. Table VI also indicates that 1 gram of LiH, uniformly distributed throughout the LiH layer, reduces the neutron dose by 7.19 x 10^{-4} rem/hr. Also shown in Table VI is the dose coefficient per centimeter for LiH. For the LiH layer this coefficient is -40.0 rem/hr/cm.

Table V gives a comparison of the fractional change in the neutron dose functional per unit change in the LiH layer thickness, $\delta F/F\delta t$, between the perturbation theory result and the result calculated by successive direct transport calculations. The perturbation theory result is -.138 cm^{-1} while the result from direct flux calculations is -.140. The two results are in excellent agreement with each other.

Effect of the Tungsten and Lithium Hydride Layers on the Photon Dose

The photon dose rate was calculated from equation (3) to be 2.59 x 10^4 rad/hr for a total secondary gamma ray source, due to neutron absorptions in W, of 3.98 x 10^{17} photons/sec. Using equation (3a) the photon dose was also calculated to be 2.59 x 10^4 rad/hr. The photon dose rate was calculated from equation (3) to be 7.10 x 10^3 rad/hr for a total secondary gamma ray source, due to neutron inelastic scattering in W, of 8.17 x 10^{17} photons/sec. Using equation (3a) the photon dose for this case was calculated to be 7.19 x 10^3 rad/hr.

Table VII presents the effect on the photon dose functionals, $4\pi\delta F$, of the tungsten layer. The data in Table VII gives the effect on $4\pi\delta F$ of each reaction which a photon can undergo with a nuclei of W; in addition, the effect on $4\pi\delta F$ of the perturbations in the secondary photon source are also given. From the data in the table it can be seen that a major contribution to $4\pi\delta F$ is due to these perturbations in the secondary photon source.

Table VIII gives a comparison of the fractional change in the photon dose functional per unit change in the W layer thickness, $\delta F/F\delta t$, between the perturbation theory result and the result calculated by successive direct transport calculations. The data in the table shows that there is excellent agreement in the values calculated by the two methods.

Table IX summarizes the results obtained for the effect of the LiH layer on the photon dose due to the two secondary gamma ray sources. From Table VIII it can be seen that the coefficient $\delta F/F\delta t$ computed by perturbation theory is in excellent

agreement with the result obtained from successive direct flux calculations.

CONCLUSIONS

In summary, the results obtained for the coefficient $\delta F/F\delta t$ by using perturbation theory for fixed sources were in excellent agreement with those obtained using successive direct transport calculations. Perturbation theory also gives a considerable amount of information concerning each reaction which a neutron or photon can undergo with the nuclei of various materials and thus add to the qualitative understanding of changes in shield design. This same information is not easily or readily obtainable from successive direct transport calculations. The extension of perturbation theory to two-dimensional geometry would pose no additional difficulties other than those of the transport solution itself.

REFERENCES:

1. Bernick, R. L.: Application of the Method of Steepest Descent to Laminated Shield Weight Optimization. Rep. NAA-SR-Memo 8181, North American Aviation, Inc. April 1963.

2. Lahti, G. P.: OPEX-II, A radiation Shield Optimization Code. NASA TM X-1769. March 1969.

3. Engle, Jr., W. W., Childs, R. L. and Mynatt, F. R.: The Design of Asymmetric 4π Shields for Space Reactors. Proc. of the National Symposium on Natural and Manmade Radiation in Space, pp. 73-77. NASA TM X-2440, Jan. 1972.

4. Lahti, G. P.: Application of the Method of Steepest Descent to Laminated Shield Weight Optimization with Several Constraints - Theory. NASA TM X-2435. Nov. 1971.

5. Lahti, G. P.: The DOPEX Code - An Application of the Method of Steepest Descent to Laminated-Shield-Weight Optimization with Several Constraints. NASA TM X-2554. May 1972.

6. Usachev, L. N.: Perturbation Theory for the Breeding Ratio and for Other Number Ratios Pertaining to Various Reactor Processes. Jour. of Nuclear Energy, Parts A/B, vol. 18, pp. 571-583, 1964.

7. Abagyan, A. A., Dubinin, A. A., Kazanskii, Yu.A., Orlov, V. V., Petrov, E. Ye and Pupko, V. Ya.: The Optimization of Nuclear Reactor Shielding Characteristics on the Basis of Variational Methods. Proc. of the Conf. on the Physics Problems of Reactor Shielding held at the Atomic Energy Research Establishment, Harwell, England, Sept. 1967. Rep. AERE-R-5773 vol. 4.

8. Lewins, J.: Developments in Perturbation Theory. Advances in Nuclear Science and Technology, edited by Paul Greebler and Ernest J. Henley, Academic Press, vol. 4. 1968.

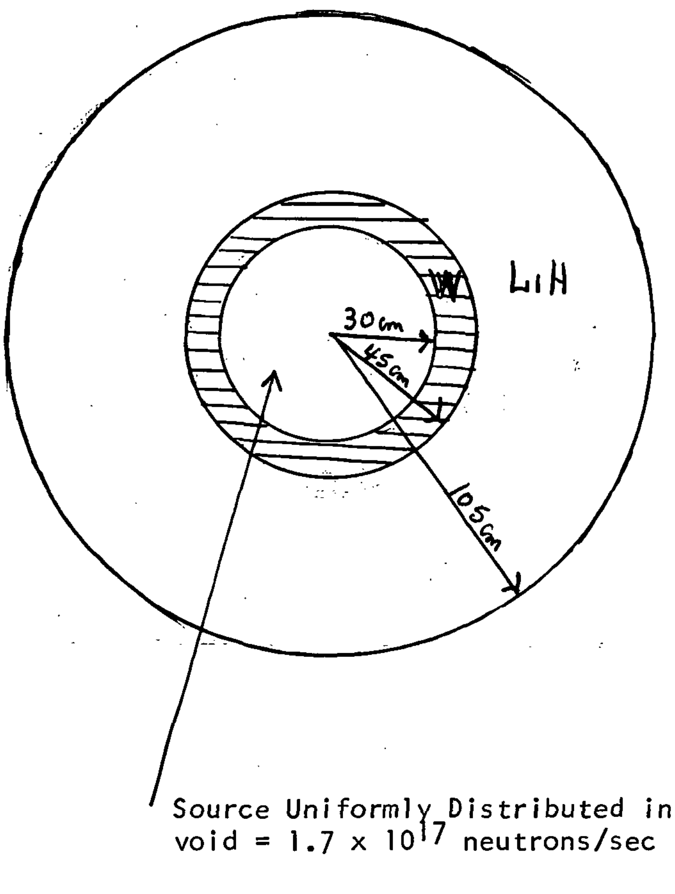

FIGURE 1. Sketch of spherical system used in illustrative problem. (The detector position is 0.25 centimeters from the boundary.)

TABLE I. Size and Composition of Spherical System

REGION	RADIUS		ELEMENT	DENSITY gm/cc	ATOM DENSITY atom/ b-cm
	Inner cm	Outer cm			
1	0	30	(void)	--	--
2	30	45	W:	19.270	.06311
			W-182	5.044	.016691
			W-183	2.765	.009100
			W-184	5.916	.019364
			W-186	5.545	.017955
3	45	105	LiH:	.74794	.056837
			H	.09437	.056837
			Li-6	.04201	.004217
			Li-7	.61156	.052620

NOTE: Detector located 0.25 centimeters from outer boundary.

TABLE II. Neutron Energy Group Boundaries, Normalized Fission Spectrum, and Neutron Flux-to-Dose Conversion Factors.

GROUP	UPPER ENERGY BOUNDARY, eV	NORMALIZED FISSION SPECTRUM	NEUTRON FLUX-TO-DOSE CONVERSION FACTOR (rem/hr)/(neuts/cm^2/sec)
1	1.492×10^{7}	.000155	1.5×10^{-4}
2	1.221 "	.000886	1.5 "
3	1.000 "	.003451	1.5 "
4	8.19×10^{6}	.018725	1.48 "
5	6.07 "	.029349	1.4 "
6	4.97 "	.047774	1.35 "
7	4.07 "	.106381	1.3 "
8	3.01 "	.088247	1.28 "
9	2.47 "	.046962	1.28 "
10	2.23 "	.095373	1.28 "
11	1.83 "	.136033	1.35 "
12	1.35 "	.080244	1.4 "
13	1.11 "	.069595	1.35 "
14	9.07×10^{5}	.127183	1.0 "
15	5.50 "	.049062	7.6×10^{-5}
16	4.08 "	.085216	5.0 "
17	1.11 "	.015364	2.0 "
18	1.50×10^{4}	0	0
19	3.35×10^{3}	0	0
20	5.83×10^{2}	0	0
21	1.01 "	0	0
22	2.90×10^{1}	0	0
23	1.07 "	0	0
24	3.06×10^{0}	0	0
25	1.13 "	0	0
26	4.14×10^{-1}	0	0

NOTE: Lower energy boundary of thermal group is 0.001 eV.

TABLE III. Photon Energy Group Structure, Secondary Photon Spectra for Tungsten, and Photon Flux-to-Dose Conversion Factors

GROUP	Upper Energy Boundary, eV	Number of Photons/abs in W	Number of Photons/inel. event in W	Photon Flux-to-Dose Conversion Factors (rad/hr)/(photons/cm^2-sec)
1	8.00×10^6	.1067	.00030	6.510×10^{-6}
2	5.50 "	.0610	.00038	5.712 "
3	5.00 "	.0547	.00042	5.345 "
4	4.50 "	.0471	.00047	4.895 "
5	4.00 "	.2000	.00053	4.513 "
6	3.50 "	.2308	.00154	4.102 "
7	3.00 "	.2071	.00714	3.697 "
8	2.60 "	.2417	.01250	3.322 "
9	2.20 "	.3250	.03000	2.913 "
10	1.80 "	.2857	.44444	2.472 "
11	1.35 "	.4444	.88889	1.883 "
12	.90 "	.7538	.07692	1.105 "
13	.40 "	.3636	.15152	5.886×10^{-7}
14	.26 "	0	0	3.240 "
15	.15 "	0	0	0

NOTE: Lower energy group boundary of group 15 is 8.0×10^4 eV.

TABLE IV. Neutron Dose Functionals and Derivatives for the Tungsten Layer

Change in Dose Functional for Each Neutron Reaction, $4\pi\delta F$, rem/hr	
Elastic scattering	-2.03×10^2
Inelastic Scattering	-6.30×10^2
(n,2n) Reaction	-1.94×10^2
Absorption	$-.07 \times 10^2$
Total Change in Dose Functionals $4\pi\delta F$, rem/hr	-10.3×10^2
Change in Dose Functional per Gram rem/hr/gm	-2.00×10^{-4}
Change in Dose Functional per cm, rem/hr/cm	-68.9

TABLE V. Comparison for the Neutron Problem of Derivative $\delta F/F\delta t$ Calculated by Perturbation Theory and Successive Direct Transport Calculations.

REGION	Fractional Increase in Density, $\delta\rho/\rho$	Equivalent Thickness, $\delta t = \frac{\delta\rho}{\rho} t$, cm	Fractional Change in Neutron Dose for Unit Change in Layer Thickness, $\delta F/F\delta t$, cm^{-1}		$\frac{\text{Pert. Calc.}}{\text{Direct Calc.}}$
			Direct Calc.	Perturbation Calc.	
W	.02	.30	-.234	-.238	1.02
LiH	.01	.60	-.140	-.138	.99

TABLE VI. Neutron Dose Functionals and Derivatives for the Lithium-Hydride Layer

MATERIAL	H	Li	LiH
Change in Dose Functional for Each Neutron Reaction, $4\pi\delta F$, rem/hr			
Elastic Scattering	-12.2×10^2	-6.99×10^2	-19.2×10^2
Inelastic Scattering	---	-4.70×10^2	-4.70×10^2
Absorption	---	$-.09 \times 10^2$	$-.09 \times 10^2$
Total Change in Dose Functional, $4\pi\delta F$, rem/hr	-12.2×10^2	-11.8×10^2	-24.0×10^2
Change in Dose Functional per Gram, rem/hr/gm	-2.90×10^{-3}	-4.04×10^{-4}	-7.19×10^{-4}
Change in Dose Functional per cm, rem/hr/cm	-20.4	-19.6	-40.02

TABLE VII. Photon Dose Functionals and Derivatives for the Tungsten Layer

Secondary Photon Source	W(n,γ) Reaction	W$(n,n'\gamma)$ Reactions
Change in Dose Functional for Each Photon Reaction, $4\pi\delta F$, rad/hr		
Scattering	-1.59×10^4	-7.20×10^3
Absorption	-1.12×10^4	-2.35×10^3
Change in Dose Functional for Secondary Source Perturbations, $4\pi\delta F$, rad/hr	-1.55×10^4	-8.80×10^3
Total Change in Dose Functional, $4\pi\delta F$, rem/hr	-4.26×10^4	-1.83×10^4
Change in Dose Functional per gram, rad/hr/gm	-8.23×10^{-3}	-3.54×10^{-3}
Change in Dose Functional per cm, rad/hr/cm	-2.84×10^3	-1.22×10^3

TABLE VIII. Comparison for Photon Problem of Derivative $\delta F/F\delta t$ Calculated by Perturbation Theory and Successive Direct Transport Calculations.

REGION	Fractional Increase in Density, $\delta\rho/\rho$	Equivalent Thickness, $\delta t = \frac{\delta\rho}{\rho} t$, cm	Fractional Change in Photon Dose per Unit Change in Layer Thickness, $\delta F/F\delta t$, cm^{-1}		Pert. Calc. / Direct Calc
			Direct Calc.	Perturb. Calc.	
Secondary Photon Source; W(n,γ) Reaction					
W	.02	.30	-.107	-.110	1.02
LiH	.01	.60	-.026	-.026	1.00
Secondary Photon Source; W(n,n′γ) Reaction					
W	.02	.30	-.168	-.172	1.02
LiH	.01	.60	-.039	-.139	1.00

TABLE IX. Photon Dose Functionals and Derivatives for the Lithium-Hydride Layer

Secondary Photon Source	$W(n,\gamma)$ Reaction			$W(n,n'\gamma)$ Reaction		
	H	Li	LiH	H	Li	LiH
Change in Dose Functional for each Photon Reaction, $4\pi\delta F$, rad/hr						
Scattering	-1.01×10^{4}	-3.02×10^{4}	-4.02×10^{4}	-4.11×10^{3}	-1.23×10^{4}	-1.64×10^{4}
Absorption	$-.77\times10^{2}$	-5.95×10^{2}	-6.72×10^{2}	-1.91	-16.2	-18.1
Total Change in Dose Functional, $4\pi\delta F$, rad/hr	-1.02×10^{4}	-3.08×10^{4}	-4.09×10^{4}	-4.11×10^{3}	-1.23×10^{4}	-1.64×10^{4}
Change in Dose Functional per gram, rad/hr/gm	-2.41×10^{-2}	-1.05×10^{-2}	-1.22×10^{-2}	-9.75×10^{-3}	-4.22×10^{-3}	-4.92×10^{-3}
Change in Dose Functional per cm, rad/hr/cm	-1.69×10^{2}	-5.13×10^{2}	-6.82×10^{2}	-68.49	-2.05×10^{2}	-2.74×10^{2}